

FULL-DEPTH COADDS OF THE WISE AND FIRST-YEAR NEOWISE-REACTIVATION IMAGES

AARON M. MEISNER^{1,2}, DUSTIN LANG^{3,4}, AND DAVID J. SCHLEGEL²

Draft version September 4, 2018

ABSTRACT

The Near Earth Object Wide-field Infrared Survey Explorer (NEOWISE) Reactivation mission released data from its first full year of observations in 2015. This data set includes ~ 2.5 million exposures in each of W1 and W2, effectively doubling the amount of WISE imaging available at $3.4\mu\text{m}$ and $4.6\mu\text{m}$ relative to the AllWISE release. We have created the first ever full-sky set of coadds combining all publicly available W1 and W2 exposures from both the AllWISE and NEOWISE-Reactivation (NEOWISER) mission phases. We employ an adaptation of the unWISE image coaddition framework (Lang 2014), which preserves the native WISE angular resolution and is optimized for forced photometry. By incorporating two additional scans of the entire sky, we not only improve the W1/W2 depths, but also largely eliminate time-dependent artifacts such as off-axis scattered moonlight. We anticipate that our new coadds will have a broad range of applications, including target selection for upcoming spectroscopic cosmology surveys, identification of distant/massive galaxy clusters, and discovery of high-redshift quasars. In particular, our full-depth AllWISE+NEOWISER coadds will be an important input for the Dark Energy Spectroscopic Instrument (DESI) selection of luminous red galaxy and quasar targets. Our full-depth W1/W2 coadds are already in use within the DECam Legacy Survey (DECaLS) and Mayall z-band Legacy Survey (MzLS) reduction pipelines. Much more work still remains in order to fully leverage NEOWISER imaging for astrophysical applications beyond the solar system.

Subject headings: methods: data analysis – surveys: cosmology – techniques: image processing

1. INTRODUCTION

The Wide-field Infrared Survey Explorer (WISE; Wright et al. 2010) has performed a full-sky imaging survey in four broad mid-infrared bandpasses centered at 3.4, 4.6, 12 and 22 microns, labeled W1-W4 from blue to red. WISE has dramatically enhanced our knowledge of the mid-infrared sky, and publicly released numerous catalog and imaging data products of high value to the astronomical community.

WISE launched in December 2009, and undertook a seven month, full-sky survey in all of W1-W4 from February 2010 through August 2010. In September 2010, the solid hydrogen cryogen used to cool the W3 and W4 instrumentation was depleted, significantly reducing the quality of W3 imaging and rendering W4 unusable. Nevertheless, WISE continued surveying the sky from September 2010 to February 2011 in W1 and W2, including a portion of the mission referred to as NEOWISE (Mainzer et al. 2011). In February 2011 WISE was placed in hibernation. In October 2013, WISE was reactivated, and recommenced surveying the sky in W1 and W2. This W1/W2 survey is referred to as NEOWISE-Reactivation (NEOWISER) and is expected to continue until 2017. The first-year NEOWISER data products, including all single-exposure images, were publicly released in March 2015. Importantly, the NEOWISER images are of very nearly the same high quality as those of the pre-

hibernation WISE mission (Mainzer et al. 2014).

Several data products consisting of full-sky, stacked WISE imaging are currently available for the first 13 months of data. The WISE team has created a set of “Atlas” coadds smoothed by the point spread function (PSF) using the first 7 months of data (the All-Sky release), and the first 13 months of data (the AllWISE release). In an independent processing effort, Lang (2014) has produced custom “unWISE” stacks analogous to the AllWISE Atlas images, but at the full spatial resolution of the instrument. These unWISE stacks are optimized for forced photometry, and have proven to be an important input for eBOSS target selection (Lang et al. 2014; Myers et al. 2015; Prakash et al. 2015).

However, until now, no full-sky set of W1/W2 coadds combining all pre and post reactivation exposures has existed. The primary motivation for such a data product is the enhanced depth achieved relative to AllWISE-only coadds. Among other benefits, this added depth will improve the utility of WISE for selecting higher-redshift spectroscopic targets, in particular for the upcoming Dark Energy Spectroscopic Instrument (DESI, Levi et al. 2013). Furthermore, folding in two additional scans of WISE data at each sky location allows time-dependent artifacts to be nulled, largely eliminating spatial nonuniformities in image quality and derivative catalogs.

Here we present a new set of full-sky coadds generated by combining all publicly available W1/W2 exposures from the AllWISE and NEOWISER programs, using an adaptation of the Lang (2014) unWISE methodology. These ‘full-depth’ coadds are publicly available online.⁵

⁵ <http://unwise.me>

¹ Berkeley Center for Cosmological Physics, Berkeley, CA 94720, USA

² Lawrence Berkeley National Laboratory, Berkeley, CA, 94720, USA

³ Department of Astronomy & Astrophysics and Dunlap Institute, University of Toronto, Toronto, ON M5S 3H4, Canada

⁴ Department of Physics & Astronomy, University of Waterloo, 200 University Avenue West, Waterloo, ON, N2L 3G1, Canada

In §2 we briefly describe the W1/W2 single-exposure data set from which our coadds are constructed. In §3, we review the important aspects of the unWISE coaddition framework we employ and list the processing features which are newly introduced in this work. In §4 we describe an empirical photometric calibration we derived in order to combine pre and post reactivation WISE images. In §5 we describe our rejection of time-dependent artifacts, particularly scattered moonlight. In §6 we describe our procedure for recovering Moon-contaminated exposures. In §7 we highlight some important aspects of the full-sky set of full-depth coadds generated by our processing. In §8 we present a catalog-level validation of the improvements in WISE depth that result from doubling the amount of W1/W2 imaging. We conclude in §9 with a brief discussion of the work which still remains to be done with existing and future NEOWISER imaging.

2. DATA

The WISE single-exposure “L1b” images represent the input data for our W1/W2 coadds. Specifically, for each L1b frameset, we make use of the per-band `-int-`, `-msk-` and `-unc-` images, which respectively give the measured sky intensity and associated per-pixel bitmask values and uncertainty estimates. We have obtained a local copy of these files for every publicly available frameset, including those from the AllWISE release (~ 2.8 M framesets) and first-year NEOWISER release (~ 2.5 M framesets). In all we have analyzed ~ 5.3 M framesets in each of W1 and W2, corresponding to a total of ~ 32 M L1b image files, ~ 71 TB of input image data and $\sim 33 \times 10^{12}$ pixels.

In addition to L1b images, we also make use of several catalog-level WISE data products. During the photometric calibration described in §4, we select sources to photometer based on the AllWISE Source Catalog (Cutri et al. 2013). Also, to flag and reject bright solar system planets (§5), we employ the WISE Known Solar System Object Possible Association List for each mission phase (Cutri et al. 2012, 2013, 2015).

3. IMAGE COADDITION METHODOLOGY

To stack the W1/W2 single exposures, we make use of the Lang (2014) unWISE coaddition framework, and perform our image processing with an adaptation of the codebase from that work. We briefly mention a few of the salient aspects of the unWISE coaddition methodology here; for a full discussion see Lang (2014).

Like the official WISE Atlas coadds, unWISE processing divides the sky into a set of 18,240 $1.56^\circ \times 1.56^\circ$ tiles arranged along iso-declination rings. Whereas the Atlas images are smoothed by the WISE PSF, the unWISE code uses Lanczos interpolation to preserve the native WISE angular resolution during coaddition, creating stacked outputs which are 2048 pixels on a side, with $2.75''$ pixels.

During the course of this work, various modifications have been made to the unWISE codebase and methodology. Here we highlight the important updates/changes:

- We include all publicly available NEOWISER W1 and W2 exposures, approximately doubling the number of input L1b frames relative to the Lang (2014) processing.

- We adopt custom zero points based on repeat photometry at the ecliptic poles. In contrast, the Lang (2014) unWISE processing adopted zero points extracted from the L1b header metadata.
- We explicitly reject exposures contaminated by the Moon and/or solar system planets. No such rejection was included in the Lang (2014) unWISE W1/W2 coadds, although these and other artifacts were addressed to some extent via general-purpose outlier rejection.
- In this work we attempt to recover Moon-affected frames by applying polynomial background level corrections to the contaminated exposures.

The outputs generated in this work follow the same data model as those of Lang (2014). For each tile, a stacked intensity image is created, as well as auxiliary maps of useful quantities such as the per-pixel inverse variance and integer coverage. Like those of Lang (2014), our coadds have units of Vega nanomaggies.

4. CUSTOM PHOTOMETRIC CALIBRATION

In order to combine frames across multiple mission phases, it is necessary to place all exposures on a common photometric calibration so that the multiplicative scalings of all input images are consistent. Each L1b image includes a `MAGZP` header keyword which gives the nominal Vega zero point of that exposure. These zero points are essentially predictions of system throughput based on predictors such as beam splitter assembly temperature, and have been found to differ by up to several percent relative to zero point variations measured empirically with single-exposure photometry of calibrator sources (e.g. Cutri et al. 2013, §V.3.a.iii.1).

We therefore sought to derive an empirical relative photometric calibration across all mission phases accurate at the sub-percent level. To do so, we analyzed repeat measurements of compact sources near the ecliptic poles, where WISE has gathered data every ~ 95 minutes throughout the entire mission. Specifically, our sample consists of moderately bright, unsaturated compact sources with $|\beta| > 85^\circ$, avoiding a wedge defined by $-90^\circ < \lambda < 25^\circ$ near the south ecliptic pole to exclude the LMC. The positions and average magnitudes of our moderately bright source sample were drawn from the AllWISE Source Catalog, selecting W1 sources with $10.6 < w1mpro < 13.1$ and W2 sources with $9.2 < w2mpro < 11.7$, always requiring `w?cc_map=0` in the band of interest.

These spatial, magnitude and flag cuts yield samples of $\sim 109,000$ ($\sim 27,000$) unique calibrator sources in W1 (W2). We perform aperture photometry using `djs_phot` with a $27.5''$ radius for each calibrator source in every L1b exposure in which it appears sufficiently far from the image boundary. This results in a catalog of ~ 45 M (~ 15 M) W1 (W2) single-epoch aperture fluxes (in units of DN), which will form the basis for our derived time-dependent zero points. The typical calibrator source contributes $\gtrsim 400$ epochs of photometry.

We desired a photometric calibration with time resolution of one day. To achieve this, we grouped our single-exposure aperture photometry measurements in two ways. First, for each unique source, we lumped all

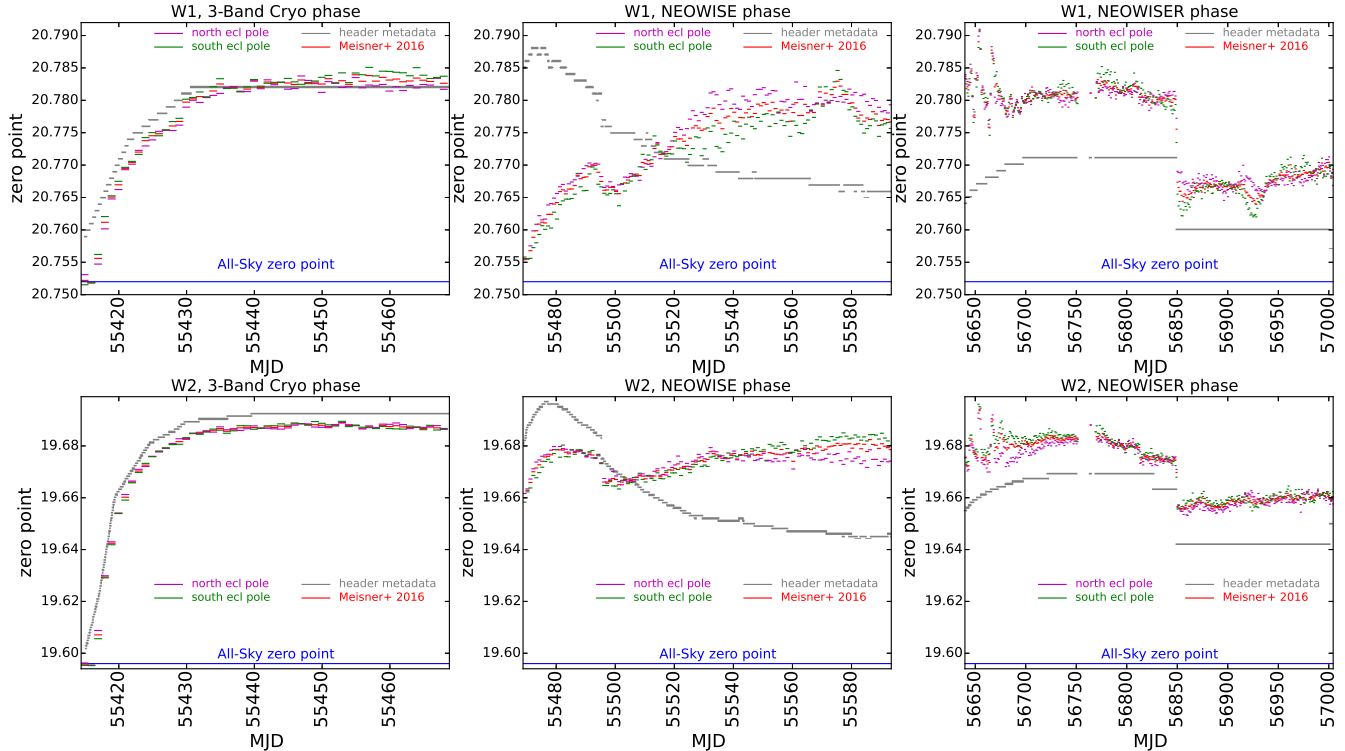


FIG. 1.— Summary of our custom photometric calibration. In each panel, the red dashes give the per-day photometric zero points we derived based on repeat measurements of stars near the ecliptic poles, as described in §4. The gray lines show the MAGZP zero point values provided by the L1b header metadata. The magenta (green) dashes represent the zero point time trends which would have resulted had we restricted our analysis to aperture photometry of only the north (south) ecliptic pole.

of its All-Sky phase measurements together to obtain its median flux (DN) in our aperture photometry system during this phase. This is justified because the All-Sky release photometric zero points are known to be remarkably stable (Jarrett et al. 2011). Indeed, using our ecliptic pole single-exposure photometry database, we were able to confirm that the All-Sky phase zero point was stable at the ≤ 2 mmag level in both bands. Next, for every aperture flux after the All-Sky phase, we calculated a multiplicative enhancement factor implied by the ratio of that measurement to the appropriate source’s median All-Sky phase flux. We then grouped these flux enhancement factors into one-day bins, and quote the median per bin as the change in multiplicative image scaling relative to the All-Sky zero point. For the All-Sky phase zero points, we adopted the MAGZP values of 20.752 in W1 and 19.596 in W2.

Figure 1 shows our derived zero points for each WISE mission phase as compared to the MAGZP values obtained from the L1b headers. In general, our per-day zero points agree reasonably well with the MAGZP values, although there are often percent-level differences, and at times disagreement at the several percent level. In some cases the empirically measured time trends within a particular mission phase show qualitative disagreement with the header metadata (e.g. both the W1 and W2 zero points during the NEOWISE mission phase). When scaling each L1b image according to its zero point during coaddition, we employ an interpolation scheme meant to avoid directly using our somewhat noisy per-day measurements. Specifically, we create a smooth approximate representation of the measured per-day zero point time-

series, based on a series of polynomials and error functions, tapering between segments such that the resulting curve is smooth.

5. REMOVING TIME-DEPENDENT ARTIFACTS

The WISE scan strategy is such that a typical sky location will be observed at approximately six month intervals, with each six-monthly “visit” yielding a series of ~ 12 exposures over a ~ 1 day time span. Within the AllWISE release, most of the sky contains just two visits of W1/W2 imaging. Incorporating exposures from both the AllWISE and NEOWISER phases effectively doubles this value to four visits everywhere on the sky. If we coadded the AllWISE+NEOWISER data naively, without concern for time dependent artifacts, we would risk corrupting regions of the sky that were pristine during the AllWISE phase. Instead, we have found that by leveraging the added redundancy of extra NEOWISER visits while carefully addressing time-dependent artifacts, we can create full-depth coadds which are nearly artifact-free over the entire sky.

The dominant time-dependent artifact in W1/W2 images is off-axis scattered light from the Moon, which can significantly contaminate images at angular separations of up to many tens of degrees. This contamination manifests itself in L1b exposures as a strongly spatially variable background level, which in certain images can be smooth, but in others can show a very complex morphology.

In the Lang (2014) unWISE processing, no steps were taken specifically to mitigate scattered moonlight in W1 and W2. However, that analysis did address Moon con-

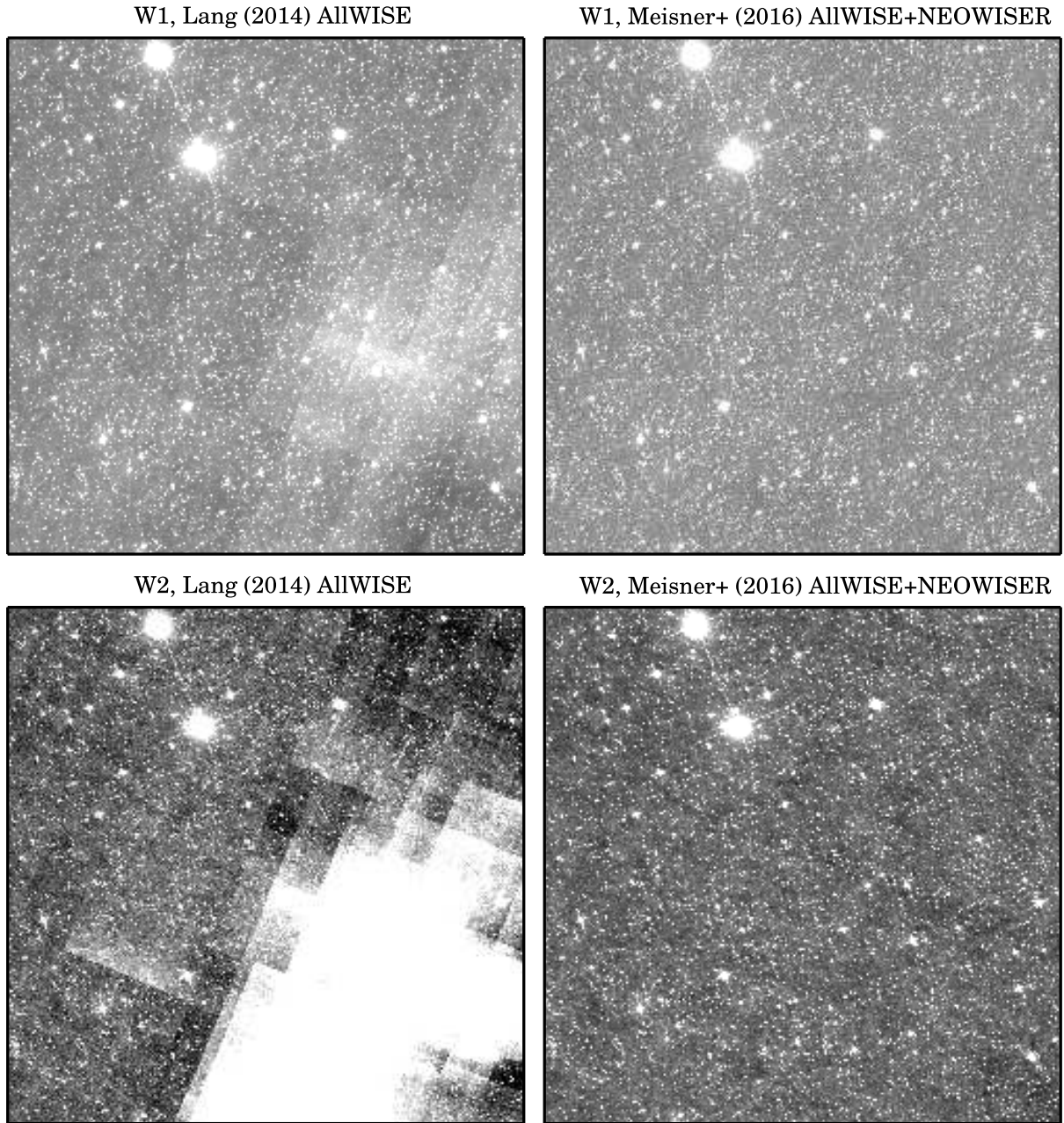


FIG. 2.— Tile 3433p000, a $1.56^\circ \times 1.56^\circ$ region of sky at low ecliptic latitude which experienced strong Moon contamination during the AllWISE mission phase. Rejecting Moon-contaminated frames as described in §5 while including two extra visits worth of NEOWISER data has dramatically improved the background level uniformity relative to the Lang (2014) version of this tile. For this tile, we were able to recover 58% (18%) of Moon-contaminated frames in W1 (W2).

tamination in W3 and W4. Lang (2014) inspected all W3/W4 exposures flagged with the `MOON_MASKED` bit, and discarded those frames with abnormally large pixel value standard deviations, indicative of a strongly varying background level (see Lang 2014 §2 for full details). In the present work we have applied this same Moon rejection criterion to W1 and W2 frames. Because of the added redundancy of two extra NEOWISER scans, we are thus able to reject many W1/W2 frames which are contaminated by moonlight, while still retaining sufficient artifact-free coverage everywhere on the sky to avoid leaving any holes in the stacks.

Figure 2 shows the dramatic improvement achieved toward maintaining a consistent coadd background level by virtue of folding in NEOWISER data and applying the frame-level Moon rejection cut, for a tile with severe Moon contamination during the AllWISE phase.

A second, less common type of time-dependent artifact results when bright solar system planets (Mars, Jupiter and Saturn) pass through the WISE field of view. These planet sightings are prominent in the Lang (2014) unWISE stacks, as no steps were taken to address such occurrences. In constructing our new full-depth coadds, we have used the Known Solar System Possible Associa-

tion List to identify all exposures in which Mars, Jupiter or Saturn fall within the WISE field of view. We discard such frames completely during coaddition and make no attempt to recover them.

Bright planets are also accompanied by scattered light halos a few degrees in size. Therefore, we additionally use ephemerides to identify all frames within 2.5° of these planets. During coaddition, such frames are initially ignored. However, we later attempt to recover such frames according to the procedure described below in §6.

6. RECOVERING CONTAMINATED FRAMES

Although we are able to dramatically reduce the impact of Moon contamination on our coadds with the exposure rejection procedure of §5, we would ideally like to recover as much Moon-contaminated data as possible, rather than simply discard it all outright. To that end, we have added an after-burner step to our coaddition procedure, during which we attempt to salvage frames that were flagged with `MOON_MASKED` and displayed abnormally large pixel value standard deviations. The procedure we employ is a variant of that described in §6.4.1 of Meisner & Finkbeiner (2014).

The first two rounds of unWISE coaddition still proceed exactly as described in Lang (2014). These steps yield a Moon-free stack which we subsequently use as a reference image to compare against, and derive low-order corrections for, each Moon-contaminated frame.

For each frame initially rejected on the basis of Moon contamination, we first resample the exposure onto the coadd astrometry. We then divide the exposure into quadrants which we analyze separately. For each quadrant, we will attempt to model the Moon contamination with a polynomial offset as a function of L1b x , y pixel coordinates. We begin by masking out the brightest and faintest 5% of pixels in the reference coadd, since pixels with bright compact sources will not be very informative for background level modeling. We then fit the difference between the masked L1b quadrant and masked reference coadd with a fourth order polynomial in L1b x , y coordinates. We evaluate the chi-squared of this model, using the reference coadd’s per-pixel standard deviation values to construct per-pixel uncertainty estimates.

For each quadrant, we deem the polynomial correction to be a satisfactory description of the scattered moonlight if the mean per-pixel chi-squared is less than 2.5. In that case, we then subtract the polynomial correction from the quadrant, and consider the quadrant “recovered”. Quadrants with poor chi-squared are discarded and remain excluded from the coadd. Once a list of all recovered quadrants has been assembled, these are accumulated into the existing reference coadd to produce a final set of outputs for the tile under consideration.

Figure 3 provides an illustration of our polynomial background modeling procedure applied to a single L1b quadrant. We were able to recover 54% of Moon-contaminated data in W1 and 33% in W2. We also apply this polynomial correction procedure to frames that we flagged as potentially affected by scattered light halos from bright solar system planets. We categorically exclude `qual_frame=0` exposures, making no attempt to recover such frames.

7. OVERVIEW OF RESULTS

Figures 4 and 5 show large-scale renderings of our full-depth coadds over portions of south Galactic cap. It is apparent that the Moon contamination has been completely eliminated in W1 and dramatically reduced in W2. It is possible that simply folding in additional NEOWISER W2 frames from forthcoming data releases will diminish the remaining Moon imprint to such an extent that no additional processing modifications will be required to address this issue.

Figure 6 shows zoom-ins of a low ecliptic latitude field, illustrating visually the reduction in statistical noise which has been achieved by doubling the number of input exposures.

Given that we imposed various frame-level cuts to eliminate time-dependent artifacts, it is reasonable to ask whether we have created any zero-coverage holes as a result. We have checked all 18,240 of our integer coverage maps, and find that every pixel has ≥ 18 epochs in W1 and ≥ 15 epochs in W2.

8. CATALOG-LEVEL VALIDATION

It is important to quantify the effect of increased coverage on the W1/W2 depths achieved by catalogs based on our AllWISE+NEOWISER coadds relative to those based on the AllWISE-only coadds of Lang (2014). A complete characterization should systematically explore a range of ecliptic and Galactic latitudes, to consider the full spectrum of interplay between decreased statistical noise and confusion. For isolated sources in the sky noise limit, we would expect a doubling of the W1/W2 imaging data to increase the depth in each band by 0.38 mag.

The only existing catalogs based on our AllWISE+NEOWISER coadds are those from DR2 of the DECam Legacy Survey⁶ (DECaLS, Schlegel et al. 2015), which include W1-W4 forced photometry for all optically detected sources. On the other hand, optical sources in DECaLS DR1 are accompanied by forced photometry of the Lang (2014) unWISE coadds. Therefore, comparing the uncertainties on W1/W2 fluxes in DR2 versus DR1 can allow us to obtain estimates of the forced-photometry depth increases for regions of low ecliptic and high Galactic latitude.

To make such a comparison, for each of W1 and W2, we select a sample of isolated DECaLS DR2 sources with `type=‘PSF’`, `wise_fracflux<0.1`, more than one DECam observation, and WISE S/N within the range 10 ± 1 . We then obtain a DR1-DR2 comparison sample by cross-matching these DR2 objects with DR1 `type=‘PSF’` sources, using a $1''$ matching radius. The resulting comparison samples have $\sim 415,000$ objects. For such sources, we find median reductions in forced photometry flux uncertainties of $1.38\times$ ($1.30\times$) in W1 (W2). The corresponding median increase in coverage is $1.9\times$ in both bands, leading us to expect a factor of $1.38\times$ decrease in flux uncertainties based purely on reduced statistical noise.

These values are not intended to represent the enhanced depths that would result from comparing WISE-only catalogs which begin with a source detection step on the WISE coadds. Since the DR2 forced photometry does not attempt to account for faint, infrared-only sources which are newly revealed in the AllWISE+NEOWISER

⁶ <http://legacysurvey.org>

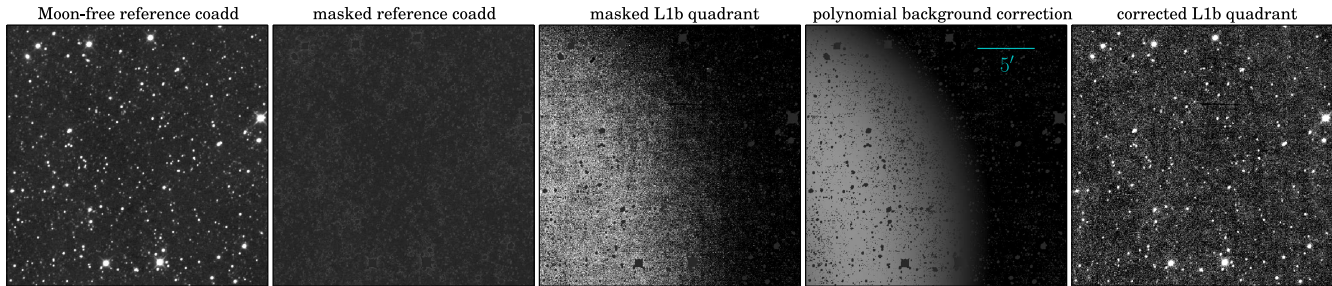


FIG. 3.— Illustration of the procedure by which we recover Moon-contaminated exposures, as described in §6. Shown here is quadrant 2 of W1 exposure 05245b140. This quadrant was successfully recovered. The polynomial background correction is subtracted from every pixel in the L1b quadrant, but is shown masked for the sake of comparison to the masked L1b quadrant.

stacks, the photometric uncertainty reduction factors we have derived serve mostly as quantitative confirmation of the decreased statistical noise shown in Figure 6.

Much more work is needed to characterize the increased sensitivity of WISE to faint infrared-only sources due to the inclusion of NEOWISER imaging, as this will inform forecasts about the final $3.4\mu\text{m}$ and $4.6\mu\text{m}$ depths expected upon WISE’s permanent retirement.

9. CONCLUSION & FUTURE WORK

We have created a full-sky set of W1/W2 coadds which combine all publicly available exposures from both the AllWISE and NEOWISER releases. Doubling the amount of WISE imaging relative to the AllWISE release has resulted in improved W1/W2 depths and allowed for the elimination of nearly all time-dependent artifacts. Our new AllWISE+NEOWISER W1/W2 coadds are publicly available via <http://unwise.me>.

Although the present analysis constituted a significant data processing endeavor, it represents only a small fraction of the work that must be done to maximize science return from the NEOWISER imaging data set. Creation of time-resolved coadds spanning the ~ 5 year AllWISE-NEOWISER time baseline would enable a wealth of important time-domain projects, ranging from brown dwarf searches to infrared quasar variability studies. As additional years of NEOWISER data become publicly available, it will be necessary to continue updating the full-depth AllWISE+NEOWISER coadds to maximize the achieved W1/W2 depths. Finally, the creation of WISE-only (as opposed to forced photometry) catalogs based on deep coadds which incorporate NEOWISER images will be needed to enable a variety of exciting discoveries.

We thank Roc Cutri for his guidance in making use of the WISE/NEOWISE data products. We thank Stephen Bailey for downloading the L1b images to NERSC. We thank Doug Finkbeiner for providing access to the big-

memory computers which were used to run coadds near the ecliptic poles. We thank Peter Nugent for data management and HPC assistance. We thank Ben Weaver, Debbie Bard and Rollin Thomas for additional HPC advice. We thank many members of the DECaLS/MzLS data team for valuable feedback, especially Arjun Dey, Doug Finkbeiner, John Moustakas, Bob Blum and Peter Eisenhardt.

This research is supported by the Director, Office of Science, Office of High Energy Physics of the U.S. Department of Energy under Contract No. DEAC0205CH1123, and by the National Energy Research Scientific Computing Center, a DOE Office of Science User Facility under the same contract; additional support for DESI is provided by the U.S. National Science Foundation, Division of Astronomical Sciences under Contract No. AST-0950945 to the National Optical Astronomy Observatory; the Science and Technologies Facilities Council of the United Kingdom; the Gordon and Betty Moore Foundation; the Heising-Simons Foundation; and by the DESI Member Institutions. The Dunlap Institute is funded through an endowment established by the David Dunlap family and the University of Toronto.

This research made use of the NASA Astrophysics Data System (ADS) and the IDL Astronomy User’s Library at Goddard.⁷

This research makes use of data products from the Wide-field Infrared Survey Explorer, which is a joint project of the University of California, Los Angeles, and the Jet Propulsion Laboratory/California Institute of Technology, funded by the National Aeronautics and Space Administration. This research also makes use of data products from NEOWISE, which is a project of the Jet Propulsion Laboratory/California Institute of Technology, funded by the Planetary Science Division of the National Aeronautics and Space Administration.

⁷ Available at <http://idlastro.gsfc.nasa.gov>

REFERENCES

- Cutri, R. M., Mainzer, A., Conrow, T., et al. 2015, Explanatory Supplement to the NEOWISE Data Release Products, Tech. rep.
 Cutri, R. M., Wright, E. L., Conrow, T., et al. 2012, Explanatory Supplement to the WISE All-Sky Data Release Products, Tech. rep.
 —. 2013, Explanatory Supplement to the AllWISE Data Release Products, Tech. rep.
 Jarrett, T. H., Cohen, M., Masci, F., et al. 2011, *ApJ*, 735, 112
 Lang, D. 2014, *AJ*, 147, 108
 Lang, D., Hogg, D. W., & Schlegel, D. J. 2014, arXiv:1410.7397
 Levi, M., Bebek, C., Beers, T., et al. 2013, arXiv:1308.0847
 Mainzer, A., Bauer, J., Cutri, R. M., et al. 2014, *ApJ*, 792, 30
 Mainzer, A., Bauer, J., Grav, T., et al. 2011, *ApJ*, 731, 53
 Meisner, A. M., & Finkbeiner, D. P. 2014, *ApJ*, 781, 5

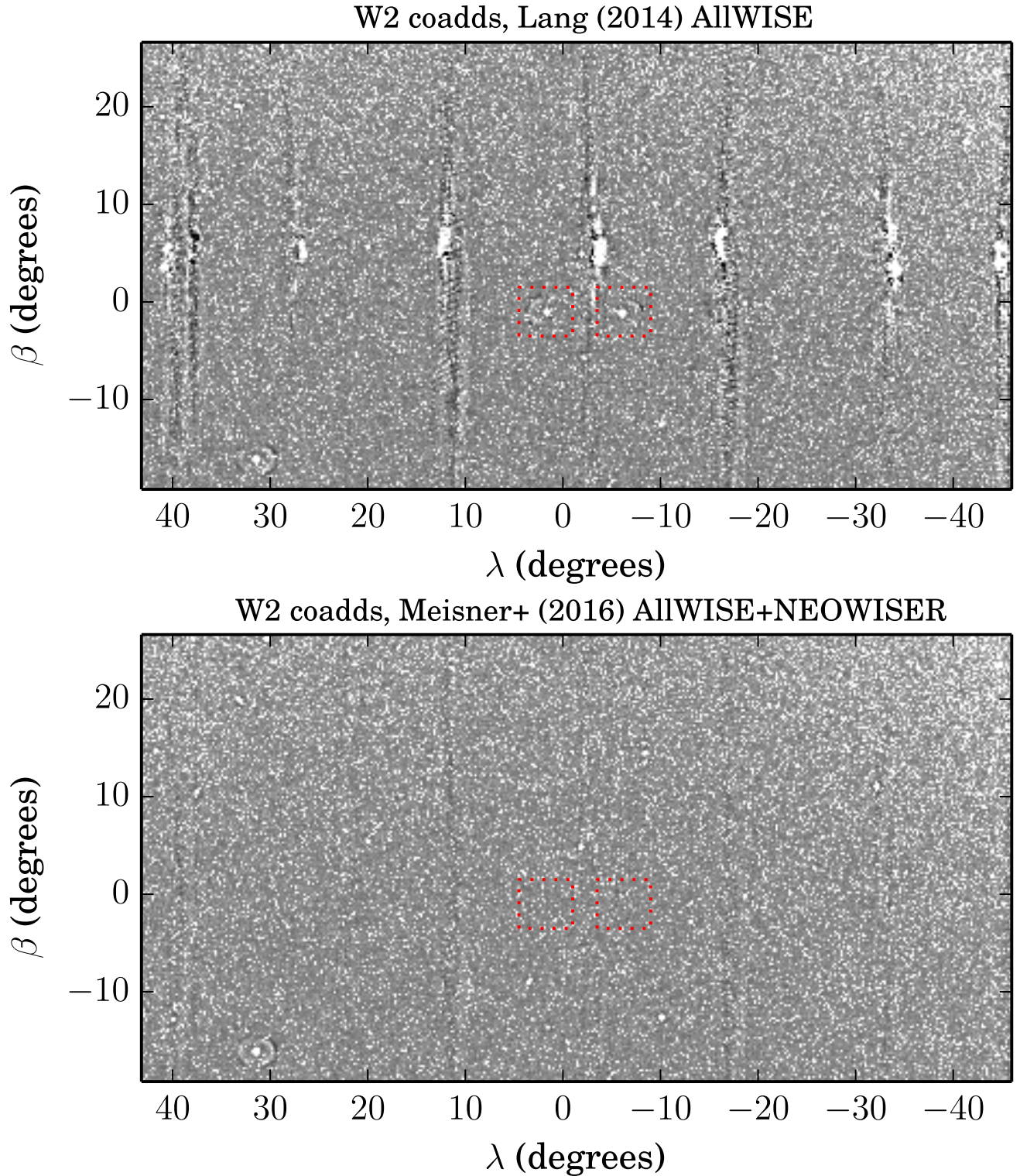


FIG. 4.— A large portion of the south Galactic cap near the ecliptic plane is shown in W2. Top: Lang (2014) unWISE coadds based on the AllWISE release imaging and without rejection of Moon-contaminated frames. Bottom: same region of sky in our new AllWISE+NEOWISER stacks, with double the redundancy in sky coverage and rejection/recovery of Moon-contaminated frames. It is clear that the scattered moonlight, which appears as a series of vertical streaks, has been largely removed in W2, although some traces still remain. The two dotted red boxes show locations where Jupiter passed through the WISE field of view. The imprints of such planet sightings have now been removed.

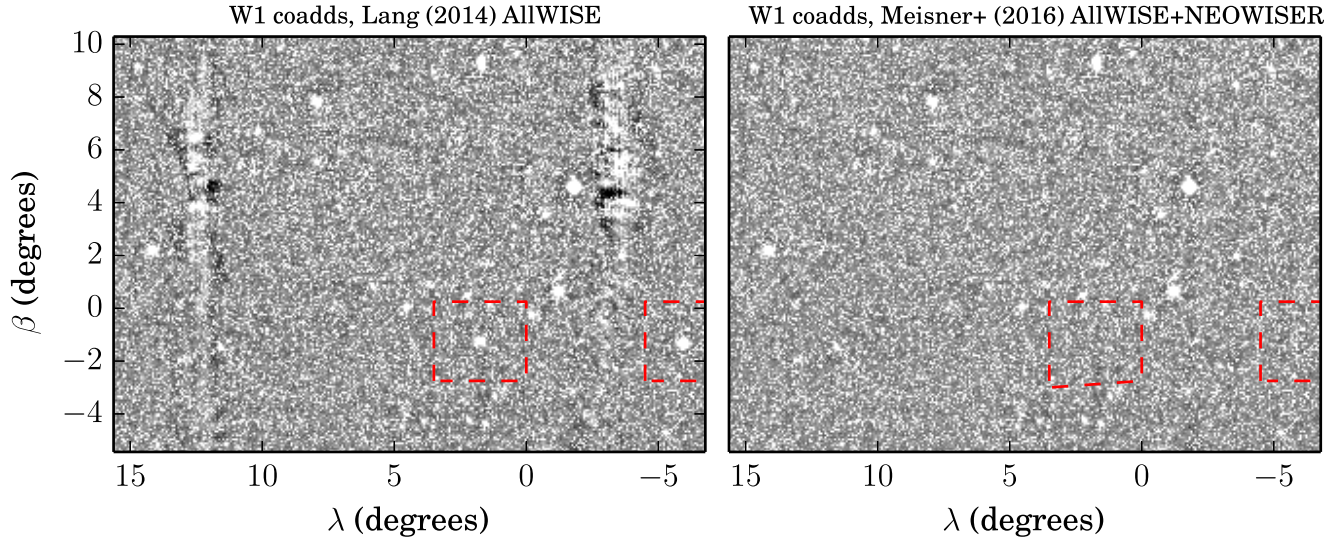


FIG. 5.— A subsection of the region displayed in Figure 4, now shown in W1. Left: Lang (2014) unWISE coadds based on the AllWISE release imaging and without rejection of Moon-contaminated frames. Right: same region of sky in our new AllWISE+NEOWISER stacks, with double the redundancy in sky coverage and rejection/recovery of Moon-contaminated frames. Scattered moonlight (vertical streaks in left panel) has been completely eliminated in W1. The two dashed red boxes show locations where Jupiter passed through the WISE field of view. The imprints of such planet sightings have now been removed

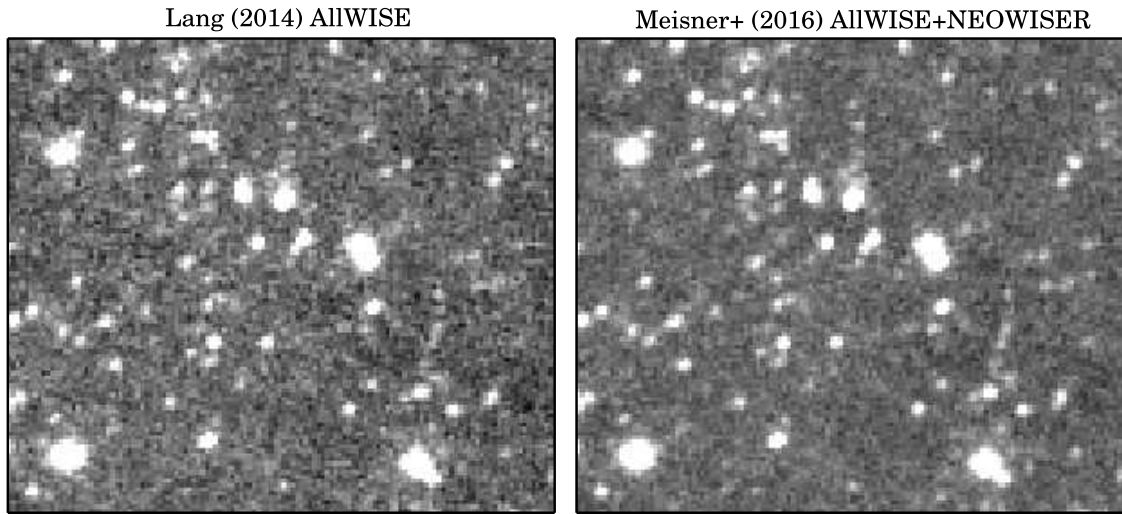


FIG. 6.— Example of decreased image noise in W1 for a $\sim 6'$ cutout extracted from tile 3353m107, centered at $(\alpha, \delta) = (335.4585^\circ, -10.5801^\circ)$. This is a representative location at low ecliptic latitude and high Galactic latitude, with $\sim 2\times$ as much coverage in our AllWISE+NEOWISER coadd relative to that of Lang (2014). Both images are rendered with identical grayscale stretches.

Schlegel, D. J., Blum, R. D., Castander, F. J., et al. 2015, in American Astronomical Society Meeting Abstracts, Vol. 225, American Astronomical Society Meeting Abstracts, 336.07
 Wright, E. L., Eisenhardt, P. R. M., Mainzer, A. K., et al. 2010, AJ, 140, 1868